4. S. A. Bowring *et al.*, *Science* **280**, 1039 (1998).
5. Y. G. Jin *et al.*, *Science* **289**, 432 (2000).
6. J. M. Mattinson, paper presented at the American Geophysical Union Meeting, San Francisco, 10 to 14 December 2001.
7. J. M. Mattinson, in preparation.
8. Z. Li *et al.*, *Dizhixue Bao* [*Acta Geol. Sin.*] **60**, 1 (1986).
9. H. Yin, K. Zhang, J. Tong, Z. Yang, S. Wu, *Episodes* **24**, 102 (2001).
10. R. S. Nicoll, I. Metcalfe, C. Wang, *J. Asian Earth Sci.* **20**, 609 (2002).
11. A. Baud, M. Magaritz, W. T. Holser, *Geol. Rundsch.* **78**, 649 (1989).
12. W. C. Sweet, Y. Zunyi, J. M. Dickins, H. Yin, in *Permo-Triassic Events in the Eastern Tethys*, W. C. Sweet, Y. Zunyi, J. M. Dickins, H. Yin, Eds. (Cambridge Univ. Press, Cambridge, 1992), pp. 1–8.
13. J. M. Mattinson, *Contrib. Mineral. Petrol.* **116**, 117 (1994).
14. D. J. Cherniak, E. B. Watson, *Chem. Geol.* **172**, 5 (2000).
15. J. K. W. Lee, I. S. Williams, D. J. Ellis, *Nature* **390**, 159 (1997).
16. K. R. Ludwig, *Geochim. Cosmochim. Acta* **62**, 665 (1998).
17. C. E. Buck, W. G. Cavanagh, C. D. Litton, *Bayesian Approach to Interpreting Archaeological Data* (Wiley, Chichester, UK, 1996).
18. C. D. Litton, C. E. Buck, *Archaeometry* **37**, 1 (1995).
19. C. B. Ramsey, *Radiocarbon* **40**, 461 (1998).
20. G. Nicholls, M. Jones, "Radiocarbon dating with temporal order constraints," *Tech. Rep. No. 407* (Univ. of Auckland, New Zealand, 1998).
21. C. Stein, paper presented at the 3rd Berkeley Symposium on Mathematical Statistics and Probability, Berkeley, December 1954, July–August 1955.
22. K. R. Ludwig, *User's Manual for Isoplot 3.00* (Berkeley Geochronology Center, Berkeley, CA, 2003).
23. M. R. Reid, C. D. Coath, T. M. Harrison, K. D. McKeegan, *Earth Planet. Sci. Lett.* **150**, 27 (1997).
24. S. J. A. Brown, I. R. Fletcher, *Geology* **27**, 1035 (1999).
25. L. Becker, R. J. Poreda, A. G. Hunt, T. E. Bunch, M. Rampino, *Science* **291**, 1530 (2001).
26. A. R. Basu, M. I. Petaev, R. J. Poreda, S. B. Jacobsen, L. Becker, *Science* **302**, 1388 (2003).
27. L. Becker *et al.*, *Science* **304**, 1469 (2004).
28. K. A. Farley, S. Mukhopadhyay, *Science* **293**, U1 (2001).
29. C. Koeberl, I. Gilmour, W. U. Reimold, P. Claeys, B. V. Ivanov, *Geology* **30**, 855 (2002).
30. P. R. Renne, Z. Zhang, M. A. Richards, M. T. Black, A. R. Basu, *Science* **269**, 1413 (1995).
31. V. E. Courtillot, P. R. Renne, *C. R. Acad. Sci. Geosci.* **335**, 113 (2003).
32. E. S. Krull, G. J. Retallack, *Geol. Soc. Am. Bull.* **112**, 1459 (2000).
33. G. Ryskin, *Geology* **31**, 741 (2003).
34. S. M. Stanley, X. Yang, *Science* **266**, 1340 (1994).
35. M. Zhou *et al.*, *Earth Planet. Sci. Lett.* **196**, 113 (2002).
36. K. Min, R. Mundil, P. R. Renne, K. R. Ludwig, *Geochim. Cosmochim. Acta* **64**, 73 (2000).
37. J. Kwon, K. Min, P. J. Bickel, P. R. Renne, *Math. Geol.* **34**, 457 (2002).
38. This study was supported by the NSF (EAR-0125799), the Australian Research Council, and the Ann and Gordon Getty Foundation. We thank J. Mattinson for generously sharing his ideas; B. Nicoll and Zhihao Wang for help and support in the field; M. Cover, A. DeHollan, and G. Johnson for lab assistance; and J. Feinberg for SEM imaging. This work is dedicated to the late Rudolf H. Steiger.

Supporting Online Material

www.sciencemag.org/cgi/content/full/305/5691/1760/DC1
Materials and Methods
Fig. S1
Table S1
References

2 June 2004; accepted 6 August 2004

Molecular Cloud Origin for the Oxygen Isotope Heterogeneity in the Solar System

Hisayoshi Yurimoto[1]* and Kiyoshi Kuramoto[2]

Meteorites and their components have anomalous oxygen isotopic compositions characterized by large variations in $^{18}O/^{16}O$ and $^{17}O/^{16}O$ ratios. On the basis of recent observations of star-forming regions and models of accreting protoplanetary disks, we suggest that these variations may originate in a parent molecular cloud by ultraviolet photodissociation processes. Materials with anomalous isotopic compositions were then transported into the solar nebula by icy dust grains during the collapse of the cloud. The icy dust grains drifted toward the Sun in the disk, and their subsequent evaporation resulted in the ^{17}O- and ^{18}O-enrichment of the inner disk gas.

Oxygen is the most abundant element in the solid phases that formed early in the solar system, and it has three stable isotopes of mass numbers 16, 17, and 18. On a three-oxygen isotope diagram, $^{18}O/^{16}O$ and $^{17}O/^{16}O$ abundance ratios of most terrestrial material constitute a line with slope of ~0.5, called the terrestrial fractionation (TF) line. This slope is due to isotope fractionation processes that depend on the mass difference between each pair of isotopes. In contrast, most meteorites have oxygen isotopic compositions that diverge from the TF line (*1*). Refractory inclusions and some chondrules in primitive meteorites have the most ^{16}O-enriched isotope compositions, shifted from the TF line with magnitudes of several percent in $^{17}O/^{16}O$ and $^{18}O/^{16}O$ ratios (*1*, *2*). Nonradiogenic effects in the other major elements (e.g., Mg and Si) in these meteorite constituents have isotope compositions close to the terrestrial compositions, and their small deviations can be explained by isotope fractionation due to thermal processes, e.g., evaporation, condensation, aqueous alteration, and low-temperature chemical reaction (*3*).

The origin of mass-independent fractionation of oxygen isotopes and the lack of such fractionation in other major elements in meteorites remains poorly understood. It cannot be due to nucleosynthetic processes or nuclear reactions that involve energetic particles from the Sun or from Galactic cosmic rays, because these processes would also change the isotopic compositions of the other elements (*1*). In addition, presolar grains enriched in ^{16}O are rare in meteorites (*4*). Although some types of molecular reactions in gaseous phases have been found to induce such mass-independent isotope fractionation in oxygen (*5*), they are observed among gas species (e.g., O_3, O_2, and CO_2) that are minor in the solar nebula (*6*). Furthermore, even if such fractionation occurs, no plausible mechanism has been proposed for trapping the fractionated products into chondrite constituents. Oxygen isotope changes due to selective ultraviolet (UV) dissociation of molecules in the solar nebula gas have been proposed (*5*, *7*, *8*); however, a mechanism for transferring these effects to the chondritic constituents has not been identified.

Recently, variations in $C^{16}O/C^{18}O$ ratio have been observed in diffuse molecular clouds (*9*, *10*). These variations are explained by selective predissociation (*11*) of $C^{18}O$ by UV radiation. In the environment of molecular clouds, predissociation due to line spectrum absorption of UV photons is the dominant mechanism for photodissociation of CO (*12–17*). UV intensity at the wavelengths of dissociation lines for abundant $C^{16}O$ rapidly attenuates in the surface layer of a molecular cloud, because of its UV self-shielding. For less abundant $C^{17}O$ and $C^{18}O$, which have shifted absorption lines because of differences in vibrational-rotational energy levels, the attenuation is much slower. As a result, $C^{17}O$ and $C^{18}O$ are dissociated by UV photons even in a deep molecular cloud interior. This process results in selective enrichment of CO in ^{16}O and enrichment of atomic oxygen in ^{17}O and ^{18}O.

Because CO and atomic oxygen are the dominant oxygen-bearing gas species in molecular clouds (*18*), their isotopic fractionation may propagate to other oxygen-bearing species. Water ice is the dominant oxygen-bearing species among ices in molecular clouds (*19*), where it nucleates and grows on silicate dust grains by surface hydrogenation reactions be-

[1]Department of Earth and Planetary Sciences, Tokyo Institute of Technology, Meguro, Tokyo 152–8551, Japan. [2]Division of Earth and Planetary Sciences, Hokkaido University, Sapporo, Hokkaido 060–0810, Japan.

*To whom correspondence should be addressed. E-mail: yuri@geo.titech.ac.jp

tween atomic oxygen and hydrogen (*20*, *21*). Therefore, oxygen isotopic compositions of H_2O ice should be close to those of gaseous atomic oxygen enriched in ^{17}O and ^{18}O (*22*). Water ice is observed in molecular clouds with total visual extinction (A_V) greater than 3.2 (*23*); abundance of water ice increases with increasing A_V (*24*). As a molecular cloud becomes dense, most of the atomic oxygen reacts to form H_2O ice, and CO becomes the most dominant gas species within 10^5 years (*25*). Thus, the oxygen isotopic composition of the gas in a dense molecular cloud becomes enriched in ^{16}O with time.

Low-mass (less than two solar masses) stars form by collapse of individual cores or clumps in a cold, dark molecular cloud with molecular densities of hydrogen (n_{H2}) of 10^4 to 10^5 cm^{-3}, A_V of 5 to 25, and temperatures as low as ~10 K (*26*). According to a model simulating photochemical isotope fractionation in a molecular cloud (*17*), under these typical cloud parameters, the isotopic compositions of ice and gas are expected to be in the ranges $\delta^{18}O_{MC} = +100$ to $+250$ per mil (‰) and $\delta^{18}O_{MC} = -60$ to -400‰, respectively, where $\delta^{18}O_{MC} \equiv \{[(^{18}O/^{16}O)/(^{18}O/^{16}O)_{MC}] - 1\} \times 1000$; $(^{18}O/^{16}O)$ and $(^{18}O/^{16}O)_{MC}$ are the isotopic ratios of corresponding chemical species and the bulk molecular cloud (MC), respectively. The degrees of fractionation for calculated $^{18}O/^{16}O$ ratios are consistent with astronomical observations (*9*, *10*). Although the lack of experimental data for $C^{17}O$ predissociation prevents us from a detailed analysis of $^{17}O/^{16}O$ fractionation, its degree is likely near that for $^{18}O/^{16}O$, because the absorption lines of these minor isotope species are unsaturated at least over several tens of A_V (*15*, *16*). Such expected similarity has been recently observed for diffuse interstellar gas (*27*).

In denser and more evolved cold molecular cloud cores, most CO may become frozen onto dust grains. Because of the low temperature, oxygen isotope exchange between CO and H_2O ices is inefficient, and the original isotope fractionation of oxygen is preserved in each phase. Transient external heating by shock waves or by other mechanisms would cause vaporization of both H_2O and CO ices and local homogenization in such a cloud. However, as long as H_2O and CO molecules do not decompose into radicals and atoms, the oxygen isotope fractionation in each molecule is probably preserved.

Here we examine how such isotopic heterogeneity in a molecular cloud may cause the variations of oxygen isotopic compositions observed in our solar system. Taking relative oxygen abundances of silicates, ice, and gas to be 1:2:3 in molecular clouds (*20*), we assumed that both $\delta^{17}O_{MC}$ and $\delta^{18}O_{MC}$ ($\delta^{17\text{ and }18}O_{MC}$) are 0‰ for silicates, +120‰ for ice, and −80‰ for gas (Fig. 1A). The $\delta^{17\text{ and }18}O_{MC}$ values for H_2O ice and CO gas were chosen to be within the simulated ranges and to conserve the mean isotopic composition of the bulk molecular cloud. The ^{16}O-depleted nature of ice relative to silicates is consistent with evidence from a primitive meteorite. The most ^{16}O-depleted known component formed in the solar system is the product of aqueous alteration of Fe,Ni-metal by H_2O in the most primitive ordinary chondrite, Semarkona (*28*).

A protoplanetary disk is formed by collapse of a molecular cloud core. In the outer region of the disk, because of low temperatures (*29*), the primordial oxygen isotopic compositions of the molecular cloud components are preserved (Fig. 1B). CO sublimes while preserving its own oxygen isotope composition outside the orbits of outer planets, even in the case of frozen CO. In the inner region of the disk, H_2O ice evaporates. During an early stage of disk evolution accompanied by vigorous gas accretion, gas-dust fractionation is probably minor, and the mean oxygen isotopic composition of the inner disk gas is reset to the value of the bulk molecular cloud, $\delta^{17\text{ and }18}O_{MC} = 0$‰. Because transient heating events, such as the formation of refractory inclusions and chondrules, were common in the inner solar nebula (*30*), silicate grains would equilibrate with such gas and have similar oxygen isotopic compositions.

As the gas accretion rate decreases, dust-gas fractionation processes begin to proceed in the disk. One such fractionation process is the dust sedimentation toward the disk mid-plane (*31*) (Fig. 1D). In addition, dust particles may preferentially migrate toward the central star (*32*), and ice in the dust evaporates after passing the snow line, releasing ^{16}O-depleted water vapor into the inner disk gas (*33*) (Fig. 1D). This increases the mean $\delta^{17\text{ and }18}O_{MC}$ of disk gas along the mixing line between the oxygen isotopic compositions of CO and of H_2O ice (Fig. 1C), correlating with the degree of H_2O enrichment relative to the H_2O/CO ratio in the parent molecular cloud (*22*). Although enrichment of H_2O by a factor of 10 is justified in the solar nebula (*34*), even moderate enrichment can produce extreme ^{17}O- and ^{18}O-enrichment of the disk gas (Fig. 2). For example, if three times the H_2O enrichment occurs (i.e.,

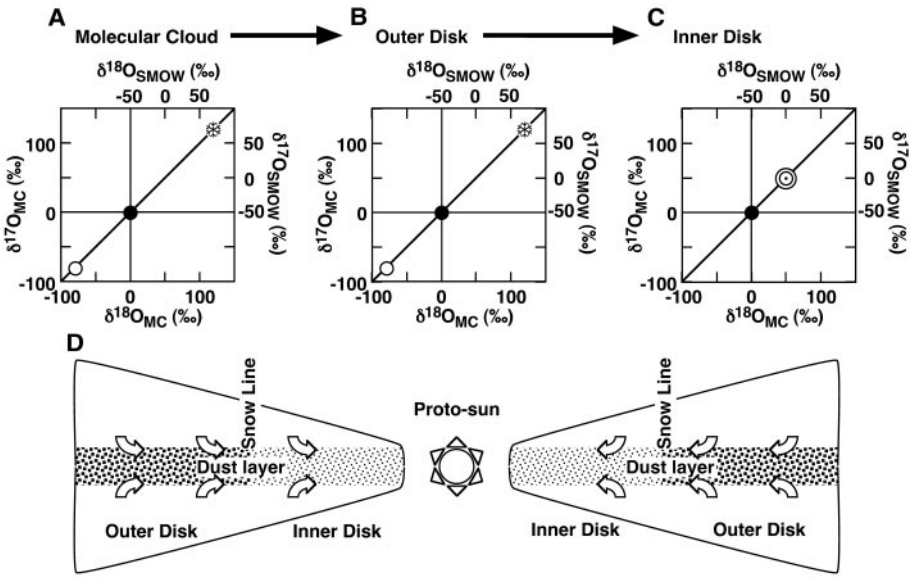

Fig. 1. Schematic diagram of oxygen isotope evolution from a molecular cloud to a protoplanetary disk with dust sedimentation. (**A**) Oxygen isotopic compositions in a molecular cloud. CO (open circle) is the most abundant species next to H_2 and He in a molecular cloud. UV radiation selectively destroys $C^{17\text{ and }18}O$, leaving behind CO enriched in ^{16}O and producing atomic oxygen enriched in ^{17}O and ^{18}O. This heavy oxygen later becomes incorporated into water ice (snowflake). $\delta^{17,18}O_{MC}$ values of 0‰, +120‰, and −80‰ for silicate (solid circles), ice, and gas, respectively, are assumed. (**B**) Oxygen isotopic compositions in the outer disk. The oxygen isotopic composition produced in the molecular cloud is preserved in the individual phases in the outer disk after accretion because of low temperature. (**C**) In the inner disk, oxygen isotopic composition of gas (⊙) shifts to a ^{16}O-poor one. (**D**) In the disk, solid materials settle down to the mid-plane and spiral into the proto-sun. Water ice evaporates inside the snow line (*29*), leading to the shift in oxygen isotopic composition shown in (C). Degrees of the shift depend on the H_2O enrichment factor (Fig. 2) and on oxygen isotopic compositions of the individual phases in the molecular cloud. The relationship between δ notation relative to SMOW and that to the molecular cloud possibly corresponds to $\delta^{17\text{ and }18}O_{SMOW} \cong \delta^{17\text{ and }18}O_{MC} - 50$‰, assuming the traditional ^{16}O-rich reservoir in the solar system. The setting of lighter silicates and heavy disk gas with respect to oxygen isotopic composition in the inner disk is consistent with meteoritic observations.

if relative oxygen abundances of ice:gas are 2:1), the mean $\delta^{17\text{ and }18}O_{MC}$ of the inner disk gas will be about +50‰. Therefore, oxygen isotopic compositions of the disk gas are altered easily by dust-gas fractionation processes (*35*). Silicate grains equilibrated with such H_2O-enriched gas during transient heating events would acquire isotope compositions with high $\delta^{17\text{ and }18}O_{MC}$ values (*36*).

Organic materials may also accommodate a significant fraction of oxygen. In hot molecular cloud cores observed for high-mass star-forming regions, CO is probably depleted because of conversion to refractory organics (*37*). Free radical reactions in ices are dominant processes to form refractory organics in molecular clouds (*38*). These organics are interpreted as UV photolysis products in H_2O ice contaminated with CO during the previous cold evolutionary stage of a molecular cloud (*20*). Because oxygen contained in such organics seems to come from H_2O and CO, its isotope composition is expected to be somewhere between those of both species, possibly $\delta^{17\text{ and }18}O_{MC}$ of +20‰ if a 1:1 contribution of H_2O and CO is assumed.

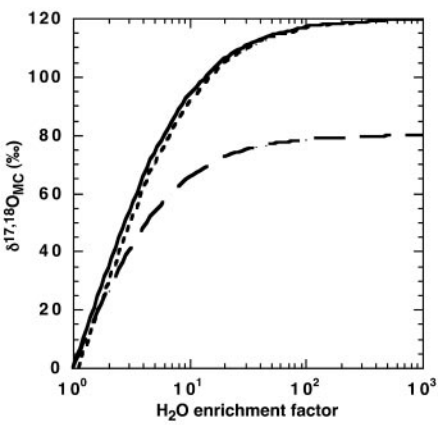

Fig. 2. $\delta^{17\text{ and }18}O_{MC}$ of inner disk gas as a function of the H_2O enrichment factor relative to molecular cloud abundance. The H_2O enrichment factor times the H_2O/CO ratio in a molecular cloud represents the H_2O/CO ratio in the disk gas, excluding chemical equilibria. The solid curve represents a case that neglects refractory organics as an oxygen carrier. Here we assume the $\delta^{17\text{ and }18}O_{MC}$ values of silicate, H_2O ice, and CO gas to be 0‰, +120‰, and −80‰, respectively, and their relative oxygen abundances in a molecular cloud to be 1:2:3. Significant ^{16}O-depletion of the gas is expected even for small H_2O enrichments. Long and short-dashed curves incorporate the effect of organics, providing that the $\delta^{17\text{ and }18}O_{MC}$ values of silicate, ice, organics, and gas are 0‰, +120‰, +20‰, and −80‰, respectively, and that the relative oxygen abundances are 1:1.5:1:2.5 in the molecular cloud. The long-dashed curve indicates the case of higher temperature than the sublimation point of organics, assuming the same enrichment factor with H_2O. The short-dashed curve indicates the case of the temperature between sublimation points of H_2O ice and of organics. In either case, significant ^{16}O-depletion of the gas occurs for small H_2O enrichment factors.

If we accept a refractory organic abundance and composition in a comet nucleus (*20*), the oxygen abundance of organics will be comparable to that of silicate (i.e., silicate:ice:organics:gas = 1:1.5:1:2.5). Because refractory organics evaporate under higher temperatures than H_2O, they may affect the mean oxygen isotopic composition of inner disk gases at high temperatures. Even though this diminishes the amount of change in the isotopic composition because of H_2O enrichment, the disk gas probably has ^{16}O-poor compositions (Fig. 2).

The proposed scenario can reproduce oxygen isotope heterogeneity in the inner solar nebula with an ^{17}O- and ^{18}O-enriched gas, i.e., ^{16}O-depleted gas, relative to silicate dust, consistent with the conventional O isotope reservoirs inferred from meteorite studies (*1*). Under such an environment, the silicate dust evolves into an ^{16}O-depleted composition through isotope exchange with the surrounding gas, because of transient heating events in the nebula. Therefore, the average oxygen isotopic composition of the solar nebula normalized to the standard mean ocean water (SMOW) may be $\delta^{17,18}O_{SMOW} \cong -50$‰ or smaller (*39*) (Fig. 1).

We have shown that even small mass fractionation for CO and atomic O in the molecular cloud can explain the formation of ^{16}O-rich or -poor reservoirs observed for the solar nebula. The ^{16}O-rion or -poor reservoirs can easily form if we use larger mass fractionation factors as expected by chemical models (*16*, *17*) and observations (*27*) of molecular clouds. Thus, the ^{16}O isotope variations may not be unique to our solar system but instead ubiquitous in any planetary system. A direct test of this scenario would be to measure the oxygen isotopic compositions of cometary ices and that of solar wind. We predict the oxygen isotopic values as $\delta^{17\text{ and }18}O_{SMOW} \cong +50$ to +200‰, −100 to −450‰, and −50‰ for cometary H_2O, cometary CO, and solar wind, respectively.

References and Notes

1. R. N. Clayton, *Annu. Rev. Earth Planet. Sci.* **21**, 115 (1993).
2. S. Kobayashi, H. Imai, H. Yurimoto, *Geochem. J.* **37**, 663 (2003).
3. R. N. Clayton, R. W. Hinton, A. M. Davis, *Philos. Trans. R. Soc. London Ser. A* **325**, 483 (1988).
4. L. R. Nittler, C. M. O. Alexander, J. Wang, X. Gao, *Nature* **393**, 222 (1998).
5. M. H. Thiemens, J. E. Heidenreich, *Science* **219**, 1073 (1983).
6. M. H. Thiemens, *Science* **283**, 341 (1999).
7. Y. Kitamura, M. Shimizu, *Moon Planets* **29**, 199 (1983).
8. R. N. Clayton, *Nature* **415**, 860 (2002).
9. C. J. Lada, E. A. Lada, D. P. Clemens, J. Bally, *Astrophys. J.* **429**, 694 (1994).
10. M. Ando *et al.*, *Astrophys. J.* **574**, 187 (2002).
11. Dissociation of a molecule occurs through its excitation to a certain bound state that is coupled to a dissociative continuum. Predissociation is caused by interaction between discrete levels of a given electronic state and the dissociative continuum of another electronic state.
12. J. Bally, W. D. Langer, *Astrophys. J.* **255**, 143 (1982).
13. Y.-H. Chu, W. D. Watson, *Astrophys. J.* **267**, 151 (1983).
14. A. E. Glassgold, P. J. Huggins, W. D. Langer, *Astrophys. J.* **290**, 615 (1985).
15. E. F. van Dishoeck, J. H. Black, *Astrophys. J.* **334**, 771 (1988).
16. S. Warin, J. J. Benayoun, Y. P. Viala, *Astron. Astrophys.* **308**, 535 (1996).
17. P. Marechal, Y. P. Viala, L. Pagani, *Astron. Astrophys.* **328**, 617 (1997).
18. P. Marechal, Y. P. Viala, J. J. Benayoun, *Astron. Astrophys.* **324**, 221 (1997).
19. Condensation temperatures of H_2O are ~90 K in a molecular cloud and ~150 K in the solar nebula, whereas those of CO are ~16 K in a molecular cloud and ~25 K in the solar nebula (*38*).
20. J. M. Greenberg, *Astron. Astrophys.* **330**, 375 (1998).
21. D. P. Ruffle, H. Eric, *Mon. Not. R. Astron. Soc.* **324**, 1054 (2001).
22. H. Yurimoto, K. Kuramoto, *Meteorit. Planet. Sci.* **37**, A153 (2002).
23. A_V is a measure used to distinguish diffuse, translucent, and dense clouds; $A_V = 2.5\log_{10}(I_{V0}/I_V)$, where I_{V0} and I_V are the intensities of visual light from a background star before and after the transverse of the cloud.
24. D. C. B. Whittet, P. A. Gerakines, J. H. Hough, S. S. Shenoy, *Astrophys. J.* **547**, 872 (2001).
25. E. A. Bergin *et al.*, *Astrophys. J.* **539**, L129 (2000).
26. E. F. van Dishoeck, G. A. Blake, B. T. Draine, J. I. Lunine, in *Protostars and Planets III*, E. Levy, J. I. Lunine, Eds. (Univ. of Arizona Press, Tucson, 1993), pp. 163–241.
27. Y. Sheffer, D. L. Lambert, S. R. Federman, *Astrophys. J.* **574**, L171 (2002).
28. B.-G. Choi, K. D. McKeegan, A. N. Krot, J. T. Wasson, *Nature* **392**, 577 (1998).
29. D. J. Stevenson, J. I. Lunine, *Icarus* **75**, 146 (1988).
30. H. C. Connolly, S. G. Love, *Science* **280**, 62 (1998).
31. S. V. W. Beckwith, T. Henning, Y. Nakagawa, in *Protostars and Planets IV*, V. Mannings, A. P. Boss, S. S. Russell, Eds. (Univ. of Arizona Press, Tucson, AZ, 2000), pp. 533–558.
32. S. J. Weidenschilling, J. N. Cuzzi, in *Protostars and Planets III*, E. H. Levy, J. I. Lunine, Eds. (Univ. of Arizona Press, Tucson, AZ, 1993), pp. 1031.
33. Because of partial support by the radial pressure gradient, disk gas tends to rotate with slightly lower velocity than the Keplerian orbital motion. This causes the frictional loss of angular momentum of immersed solid particles in the disk gas, resulting in their inward migration. The migration speed depends on the particle size and reaches a maximum of ~100 m/s at about a meter in diameter (*32*). The inward radial velocity of gas (v_g) can be estimated from mass accretion rate $\dot{M}$ as $v_g = \dot{M}/(2\pi R\Sigma)$ where R is the distance from the disk center and Σ is the gas column density. Taking $\dot{M} = 10^{-8}$ solar masses per year, which is typical for the disks around classical T-Tauri stars (*40*), and $\Sigma = 3 \times 10^3$ kg/m^3 at $R = 3$ astronomical units of the minimum-mass solar nebula (*41*), $v_g = \sim 0.1$ m/s. In such a disk, the inward radial velocities of solid particles as small as ~1 mm could be several times faster than v_g. Relative motions between the snow line and gas-dust during the disk evolution will also influence the amount of H_2O enrichment in the inner disk. As the disk accretion decays, the snow line would move inward because of disk cooling and in some cases pass the migrating solid particles. However, the snow line cannot enter a warm zone determined by the radiative heating from the central star. Thus, the inward particle migration across the snow line seems to occur unavoidably during disk evolution. Alternatively, H_2O vapor could be depleted from the inner disk if the diffusive outward transport of H_2O vapor and the cold trap outside the snow line are effective (*29*). However, because molecular diffusion is extremely slow, the main mechanism of the outward transport should be the turbulent diffusion. The turbulent flow also causes the inward gas flow because of associated turbulent viscosity. Taking into account the inward gas flow, H_2O vaporized from the solid component migrating inward is eventually supplied into the inner disk. The cold trap mechanism can work only when the solid component is sequestered into bodies

larger than kilometer-size, which have negligible radial drift. Therefore, H_2O enrichments in the inner disk would be expected before the appearance of kilometer-size bodies in the outer disk.
34. J. N. Cuzzi, K. J. Zahnle, *Astrophys. J.*, in press.
35. Recently, UV dissociation of CO at high altitudes in the disk has been numerically estimated (*42*). Lyons and Young assume H_2O ice as a carrier of the ^{16}O-poor oxygen formed by their photodissociation process to generate ^{16}O-poor gas in the disk midplane similar to an idea that we had presented in our preliminary study (*22*). However, the degree of fractionation by the disk photochemistry is dependent on many unconstrained factors, including far-UV flux, the intensity of vertical eddy mixing, and the efficiency of H_2O formation. A more detailed study coupled with disk dynamics is needed to evaluate the contribution of their CO dissociation at high altitudes in the disk to oxygen isotopic heterogeneity observed in the solar system.
36. The bulk differences in oxygen isotopic composition observed among the meteorite groups and planets (*1*) could be explained by accretion at different times or by the incorporation of different amounts of nonvaporized water ice and solids with different degrees of the solid-gas equilibration. The solid-gas equilibration and the evolution of oxygen isotopic compositions of the gas in the inner region of the disk may have been recorded by refractory inclusions and chondrules in primitive meteorites.
37. S. Kurtz, R. Cesaroni, E. Churchwell, P. Hofner, C. M. Walmsley, in *Protostars and Planets IV*, V. Mannings, A. P. Boss, S. S. Russell, Eds. (Univ. of Arizona Press, Tucson, 2000), pp. 299–326.
38. W. D. Langer *et al.*, in *Protostars and Planets IV*, V. Mannings, A. P. Boss, S. S. Russell, Eds. (Univ. of Arizona Press, Tucson, 2000), pp. 29–57.
39. We use this value according to the traditional ^{16}O-enrichment observed in most Ca-A1–rich inclusions (*1*). Recently, a chondrule having twice the traditional enrichment ($\delta^{17 \text{ and } 18}O_{SMOW}$ of about –75‰) has been reported (*2*). Although such chondrules are rare, its least fractionated bulk chemical composition from the solar abundance suggests that the average oxygen isotopic composition of silicate in the solar system was originally more enriched in ^{16}O than the traditional value. According to our model, such an extreme ^{16}O-rich chondrule is interpreted as a closer representation of the pristine solar nebula value, implying that the ordinary refractory inclusions are no longer representative of the bulk solar nebula but moderately reprocessed by the interaction with the ^{17}O- and ^{18}O-rich H_2O.
40. N. Calvet, L. Hartmann, S. E. Strom, in *Protostars and Planets IV*, V. Mannings, A. P. Boss, S. S. Russell, Eds. (Univ. of Arizona Press, Tucson, 2000), pp. 377–399.
41. C. Hayashi, K. Nakazawa, Y. Nakagawa, in *Protostars and Protoplanets II*, D. C. Black, M. S. Matthews, Eds. (Univ. of Arizona Press, Tucson, 1985), pp. 1100–1153.
42. J. R. Lyons, E. D. Young, *Lunar Planet. Sci.* **35**, 1970 (2004).
43. We thank T. J. Fagan, A. N. Krot, and E. R. D. Scott for helpful discussion and improvement of the English and two anonymous reviewers for helpful comments. Supported by Monbu-Kagaku-sho grants.

2 June 2004; accepted 2 August 2004

Middle Miocene Southern Ocean Cooling and Antarctic Cryosphere Expansion

Amelia E. Shevenell,* James P. Kennett, David W. Lea

Magnesium/calcium data from Southern Ocean planktonic foraminifera demonstrate that high-latitude (~55°S) southwest Pacific sea surface temperatures (SSTs) cooled 6° to 7°C during the middle Miocene climate transition (14.2 to 13.8 million years ago). Stepwise surface cooling is paced by eccentricity forcing and precedes Antarctic cryosphere expansion by ~60 thousand years, suggesting the involvement of additional feedbacks during this interval of inferred low-atmospheric partial pressure of CO_2 (pCO_2). Comparing SSTs and global carbon cycling proxies challenges the notion that episodic pCO_2 drawdown drove this major Cenozoic climate transition. SST, salinity, and ice-volume trends suggest instead that orbitally paced ocean circulation changes altered meridional heat/vapor transport, triggering ice growth and global cooling.

The middle Miocene climate transition (MMCT), 14.2 to 13.8 million years ago (Ma), is one of the three major steps in Earth's Cenozoic climate evolution (*1–3*). The ~1‰ increase in the oxygen-isotopic composition ($\delta^{18}O$) of benthic foraminifera describes a combination of Antarctic ice growth and global cooling at ~14 Ma, as is also indicated by Southern Ocean ice-rafted detritus, eustatic change, and the fossil record (*1–6*). However, because $\delta^{18}O$ records both temperature and global ice volume, fundamental questions and uncertainties exist concerning the magnitude and phasing of middle Miocene ice growth and cooling. The development of Mg/Ca, an independent paleotemperature proxy measured on the same foraminiferal calcite ($CaCO_3$) as $\delta^{18}O$, has facilitated isolation of the ice-volume component of $\delta^{18}O$ records (*7–12*). The Mg/Ca content of foraminifera increases exponentially with temperature (~9 ± 1% per 1°C) and is relatively insensitive to salinity and ice-volume fluctuations (*7*, *8*). Low-resolution paired benthic foraminifer Mg/Ca and $\delta^{18}O$ studies designed to constrain the timing and magnitude of pre-Quaternary ice-volume fluctuations suggest substantial Antarctic ice growth (~0.85‰) and a concomitant deep ocean cooling (2°C to 3°C) during the MMCT (*11*, *12*). The magnitude of Antarctic ice growth and rapidity of this climate transition [<0.5 million years (My)] suggests that Earth's climate system was highly sensitive to oceanic, atmospheric, and cryospheric feedbacks.

Ocean circulation and atmospheric pCO_2 variations are often cited as potential catalysts of the MMCT (*13–17*). Large-scale reorganizations of ocean circulation driven by atmospheric circulation changes and/or tectonic reorganizations of gateway regions may have altered poleward heat and moisture transport, resulting in Antarctic ice growth and global cooling (*13–15*). Ocean circulation hypotheses are supported by $\delta^{13}C$ proxy evidence (*14*, *15*, *18*, *19*) and the timing of tectonic events in the eastern Tethys/Indonesia (*4*, *20*) and the North Atlantic (*13*). Alternatively, atmospheric pCO_2 drawdown, through organic carbon sequestration on the mid-latitude continental margins (*16*) and/or enhanced silicate weathering rates (*17*), may have driven Antarctic ice-sheet expansion and cooling at ~14 Ma. Support for this "Monterey Hypothesis" comes from thick, organic carbon-rich Miocene sedimentary sequences around the Pacific Rim (*4*, *16*) and a corresponding ~ 1‰ increase in global deep sea $\delta^{13}C$ (*4*, *16*, *21*, *22*). A potential complication of the hypothesis is revealed by paleo-pCO_2 estimates (*23–25*), which indicate that atmospheric pCO_2 levels declined >3 My before the MMCT and provide little support for either elevated atmospheric pCO_2 during the warm Miocene climatic optimum (MCO) (17 to 14 Ma) or a semipermanent atmospheric pCO_2 decrease at the MMCT. These estimates indicate that factors other than those related to global carbon cycling may contribute to this major Cenozoic climate transition. To evaluate the processes and feedbacks involved in the MMCT, detailed information is needed regarding the phasing of carbon cycling, Antarctic ice growth, and high-latitude oceanic/atmospheric cooling. Acquiring this information has thus far proven difficult because of the limited availability of $CaCO_3$-rich Southern Ocean sediments and the lack of an unambiguous paleotemperature proxy.

Here, we present an independent record of middle Miocene high-latitude Southern Ocean sea surface temperature (SST). To establish the thermal and hydrographic response of Southern Ocean surface waters and the phasing of high-latitude SST change, Antarctic cryosphere expansion, and global carbon cycling between ~17 and 13 Ma, we

Department of Geological Sciences and Marine Science Institute, University of California, Santa Barbara, CA 93106–9630, USA

*To whom correspondence should be addressed. E-mail: ashevenell@umail.ucsb.edu